JOURNAL OF ELECTROMAGNETIC ENGINEERING AND SCIENCE, VOL. 15, NO. 1, 31~36, JAN. 2015

http://dx.doi.org/10.5515/JKIEES.2015.15.1.31
ISSN 2234-8395 (Online) · ISSN 2234-8409 (Print)

GA-Optimized Compact Broadband CRLH Band-Pass Filter Using Stub-Inserted Interdigital Coupled Lines

Jinsu Jeon · Sungtek Kahng* · Hyunsoo Kim

Abstract

The design of a new compact band-pass filter is proposed, which is based on the microstrip composite right- and left-handed transmission-line (CRLH-TL) structure. Particularly, the interdigital coupled (IDC) lines of the CRLH geometry are proposed to be parted by inserting open stubs to meet the specifications on the passband. In addition, there is another pair of stubs to complete the design in a limited space. These are considered in the TL-based analysis and the design parameters are calculated by genetic algorithm optimization. The measurement is shown to be acceptable and agreeable with the circuit and electromagnetic field simulations. In addition, the zeroth-order resonance (ZOR) phenomenon is verified.

Key Words: Broadband, CRLH-Metamaterial, Interdigital Coupled Lines, Optimization, Stub-Inserted.

I. INTRODUCTION

In recent years, numerous studies have been conducted to exploit the benefits of broadband communication since LTE service began to enable carriers and terminals to transmit and receive hundreds of Mbps of data, as well as to step forward to realize a Gbps data transmission would lead to 5G services. As one of many such research activities, the methods of designing band-pass filters (BPFs) have been reported to keep abreast of evolving wireless communication systems equipped with multi-function antennas and circuitry as well [1−5].

Ishida and Araki [1] designed a very wide-band BPF whose bandwidth is formed by adding zeros in the sections of the transmission line (TL). Its frequency response has notches only at the band edges and has an extremely narrow stopband. Wang et al. [2] presented the microstrip-and-CPW BPF for broadband applications, which is based on the multi-mode resonator (MMR) in the form of multiples of a quarter wavelength to broaden the bandwidth and obtain an enlarged rejection region. The idea of the MMR of the half wavelength is also used in [3], where the coupled lines of a quarter wavelength are used as the inverter. This work demonstrates the extension of the lower and higher stopbands owing to increased coupling. A composite wide-band filter was designed by Menzel et al. [4] by combining low- and high-pass filters as suspended stripline structures with different planes. Independently, Hsu et al. [5] presented composite microstrip filters for high-speed communication applications, where seven or eight TL sections of about a quarter wavelength are sequentially connected.

Recently, we suggested the design of a novel wide-band filter based on the composite right- and left-handed transmission line (CRLH-TL) metamaterial [6]. Contrary to the reference [6], we propose the use of one segment (smaller than one quarter wavelength) to make the component very compact. Besides, instead of mixing two types, for instance, as a hybrid of the microstrip and CPW, we use only the microstrip whose fabrication is inexpensive. Especially, in our proposed CRLH BPF geo-

Manuscript received November 14, 2014 ; December 23, 2014 ; Accepted January 8, 2015. (ID No. 20141114-060J)
Department of Information and Telecommunication Engineering, Incheon National University, Incheon, Korea.
*Corresponding Author: Sungtek Kahng (e-mail: s-kahng@incheon.ac.kr)

metry, we separate the interdigital coupled (IDC) lines by inserting open stubs between and grounded stubs to form a 1.7-GHz bandwidth. Furthermore, out of the CRLH unit, we place another pair of open stubs to improve the passband performance. The proposed filter, whose size is less than 1 × 1 cm^2, is fabricated and measured to be proven acceptable for the specifications.

II. Design of the CRLH-TL Type UWB BPF

The conventional CRLH-TL is a periodic structure with multi-cells, as shown in Fig. 1 [6]. The *i*-th cell consists of (C_{Li}, L_{Li}) for the left-handed and (C_{Ri}, L_{Ri}) for the right-handed properties. However, Fig. 1 should be changed to 1 cell version for effective miniaturization in Fig. 2. As well, it is in the form of a Pi-symmetric equivalent circuit.

The lumped elements of the 1-cell CRLH-TL are obtained to generate a center frequency f_0 at 4 GHz and the band edges f_R and f_L at 3.2 GHz and 4.8 GHz, respectively. Considering the balanced condition [6], f_0 is equal to the zeroth-order resonance (ZOR) point of the CRLH metamaterial line, the following formulas are used to obtain circuit elements.

$$f_L = \frac{1}{2\pi\sqrt{L_{Li}C_{Li}}}, \quad f_R = \frac{1}{2\pi\sqrt{L_{Ri}C_{Ri}}}$$
$$f_{sei} = f_{shi} = f_O, \quad f_O = \sqrt{f_L f_R} \tag{1}$$

where

$$f_{sei} = \frac{1}{2\pi\sqrt{L_{Ri}C_{Li}}}, \quad f_{shi} = \frac{1}{2\pi\sqrt{L_{Li}C_{Ri}}}.$$

Although, we use the Fig. 2 circuit, as it will change in the physical implementation, and we propose a new and hybrid-physical geometry, which will be explained later.

As it comprises the lumped elements and TL seg-ments, it is called a hybrid-physical circuit. The values of the CRLH-TL BPF with open stubs are calculated as follows to achieve the objectives in Table 1A.

Fig. 2 is related to Fig. 3 through the pi-shaped IDC lines flanked with shorted stubs appearing in [7, 8]. One block of the IDC lines is equally divided into the upper and lower blocks of the IDC lines (represented by Cs_1 as part of C_{Li}) to make room

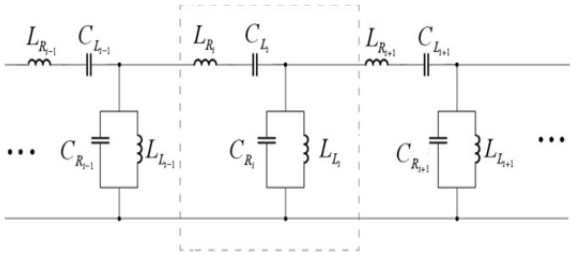

Fig. 1. Circuit model of the periodic CRLH-TL.

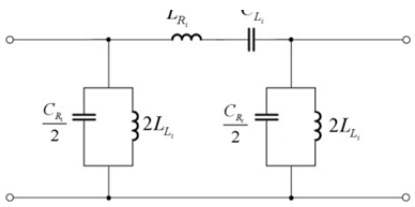

Fig. 2. Pi-equivalent circuit of the 1-cell CRLH-TL.

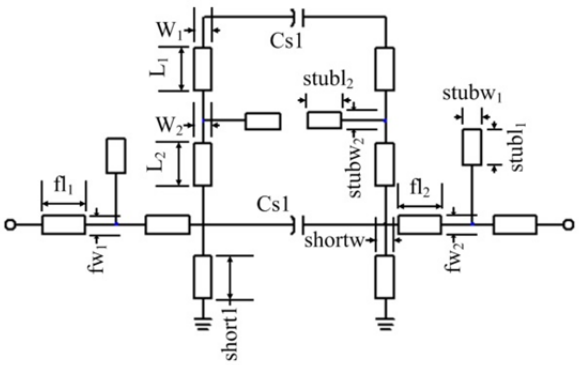

Fig. 3. Circuit model of our proposed filter geometry.

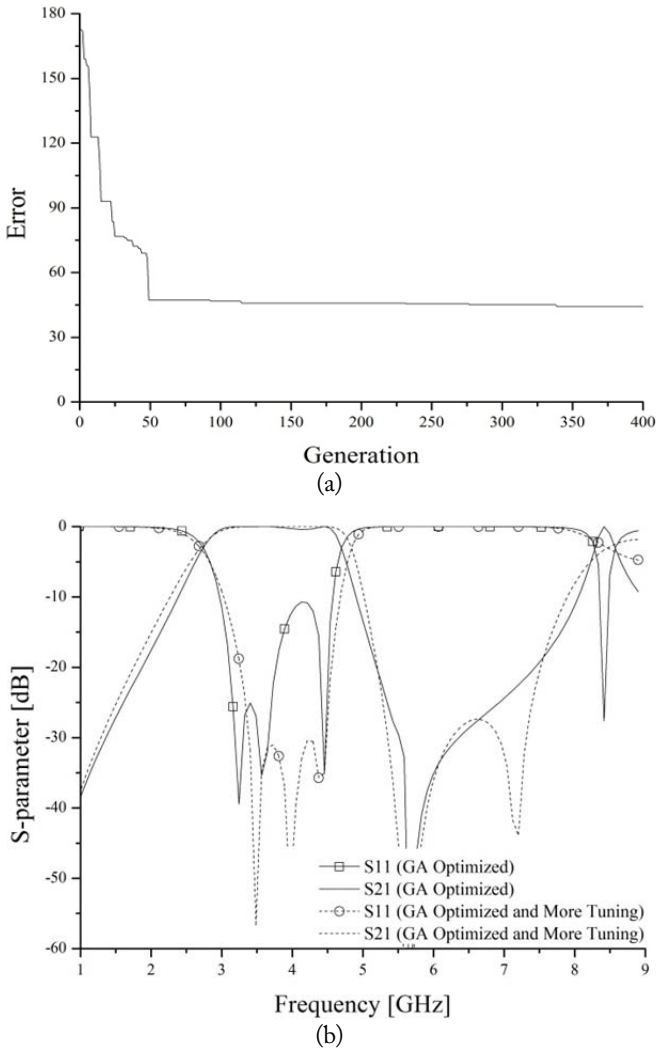

Fig. 4. Frequency responses of the prototype.

Table 1A. Design goal of this filter: lower half of the UWB

Passband (GHz)	Stopband (GHz)
$3.2 \leq f \leq 4.8$	$f < 3.2$ and $f > 4.8$
$S_{11} \leq -15$ dB	$S_{21} \leq -20$ dB
$S_{21} \geq -1$ dB	($S_{21} \leq -25$ dB @5.4 GHz)

Table 1B. Initial values of the elements for the circuit above

Parameter	Value
fw_1	1.6 mm
fl_1	1 mm
fw_2	0.1 mm
fl_2	0.7 mm
W_1	0.1 mm
L_1	0.8 mm
W_2	0.1 mm
L_2	1.5 mm
$stubw_1$	0.2 mm
$stubl_1$	7.9 mm
$stubw_2$	0.1 mm
$stubl_2$	1.4 mm
$shortw$	0.2 mm
$short_1$	1.9 mm
Cs_1	0.35 pF

for IDC open stubs as tuning elements. L_{Li}, C_{Ri}, and L_{Ri} are embedded in TL segments as in [7, 8]. As new elements, the IDC splitting open stubs are for removing the upper-half range from the full ultra-wideband (UWB), and the open stubs at the ports are for enhancing the attenuation level in the stopband and the impedance matching at the ports. Taking advantage of these elements and their genetic algorithm (GA)-optimized values, the Fig. 3 circuit with 1 results in the frequency response in Fig. 4. The binary GA is used with a 0.5 crossover, a 0.1 mutation rate, 15 parameters, 5 bits per parameter and 80 individuals through 400 generations, and it converges to the solution after the 50th generation, as presented in Fig. 4(a). All the results in Fig. 4(b) are from the circuit simulation. The scattering parameters show that the passband transitions from 3.2 to 4.8 GHz, and the insertion and return loss appear ideally good (less than 1 dB and less than 15 dB, respectively). For the final realization, the lumped capacitors Cs_1 in Fig. 3 are replaced by the IDC below.

Even if the IDC line has been around for some time, as stated before, its geometric parameters will be explored to find the desired effective inductance L_{Ri} as well as C_{Li} in our design, which differs from the others. The geometry of an n_{IDF}-fingered IDC line is described with W, l, and S denoting the finger width, the finger length. and the spacing between the two adjacent fingers, respectively. The capacitance of Fig. 5 is given as follows:

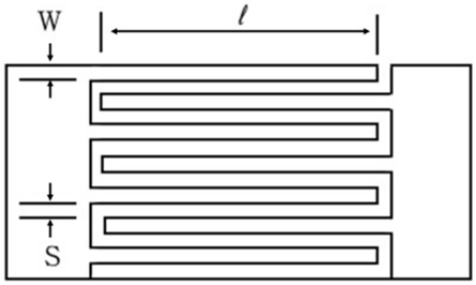

Fig. 5. Microstrip interdigital coupled (IDC) lines.

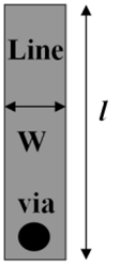

Fig. 6. Grounded microstrip line stub for inductance.

$$C(pF) = \frac{\varepsilon_{re} 10^{-3}}{18\pi} \frac{K(k)}{K'(k)} (n_{IDF} - 1)\ell \tag{2}$$

where

$$k = \tan^2\left(\frac{a\pi}{4b}\right), \quad a = \frac{W}{2}, \quad b = \frac{W+S}{2}.$$

$K(\cdot)$ and $K'(\cdot)$ are the complete elliptic integral of the first kind and its complement. Along with the series IDC, the grounded stub as the shunt inductor plays an important role. This can be realized with the following structure.

The expression as follows is commonly used for the inductance of Fig. 6 (L_{Li}) and each finger in Fig. 5 (L_{Ri}). Though it is an approximate formula, it helps us quickly approach the initial size.

$$L(nH) = 2 \times 10^{-4} l[\ln(\frac{l}{W+t}) + 1.193 + 0.224\frac{W+t}{l}] \cdot K_g \tag{3}$$

where

$$K_g = 0.57 - 0.145\ln(\frac{W}{h}),$$

where h and t above mean the thickness of the substrate and metallization in use. The expressions for the other circuit elements are found in [9], as well as a conversion between the TL segment geometry and the corresponding circuit elements, and they are used to correct the electrical behaviors based on Eqs. (2) and (3). With all these values, the physical sizes are iteratively exploited until the acquisition of the desired performance.

III. Result of Implementation

Table 2. Initial values of the elements of the proposed geometry

Parameter	Value (mm)	Parameter	Value (mm)
L_1	1.5	L_8	1.
L_2	3.7	L_9	0.9
L_3	4.5	L_{10}	4.0
L_4	3.1	L_{11}	3.6
$L_{4.1}$	1	W_1	0.1
$L_{4.2}$	2.1	W_2	0.2
L_5	5.065	W_3	0.2
L_6	1.925	W_6	0.478
$L_{6.1}$	1.3	Gap_1	0.2
L_7	0.8	Gap_2	0.1

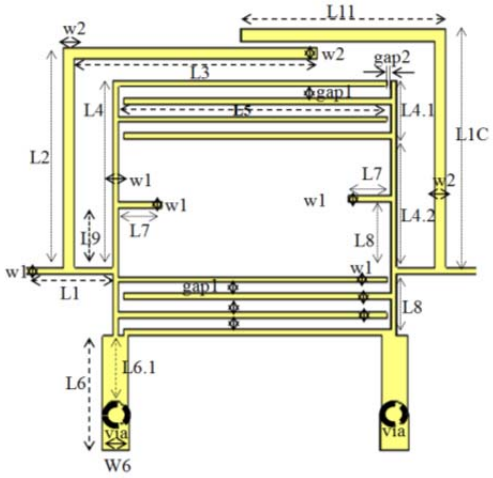

Fig. 7. Finalized version of our proposed geometry.

First, the interdigital capacitor's size is calculated to realize a capacitance of 0.35 pF. As a result, the finalized geometry and all its physical dimensions are shown in Fig. 7 and Table 2.

With the structure above, we use FR4 (ε_r = 4.4) as the substrate and 4 GHz as f_0. Based on the input for the geometry, a 3D electromagnetic field simulation has been carried out to predict the real performance and to conduct a comparison with the measurement.

Fig. 8 plots the circuit and 3D field-simulated scattering parameters S_{11} and S_{21}, which are validated by the measurement. An excellent agreement is shown between the simulated and measured S_{21} with almost the same shape of data curve, a bandwidth over 3.2 GHz through 4.8 GHz, and a insertion loss less than 1 dB (≈0.92). In addition, a good return loss lower than 15 dB is given, despite the small discrepancy due to the mechanical tolerance error. Next, from the analysis point of view regarding the design result above, we must verify the overall size as well as the ZOR of the CRLH property of this proposed geometry.

As the basis of our proposed geometry is the CRLH-TL, the metamateial property can be proven by watching the electric

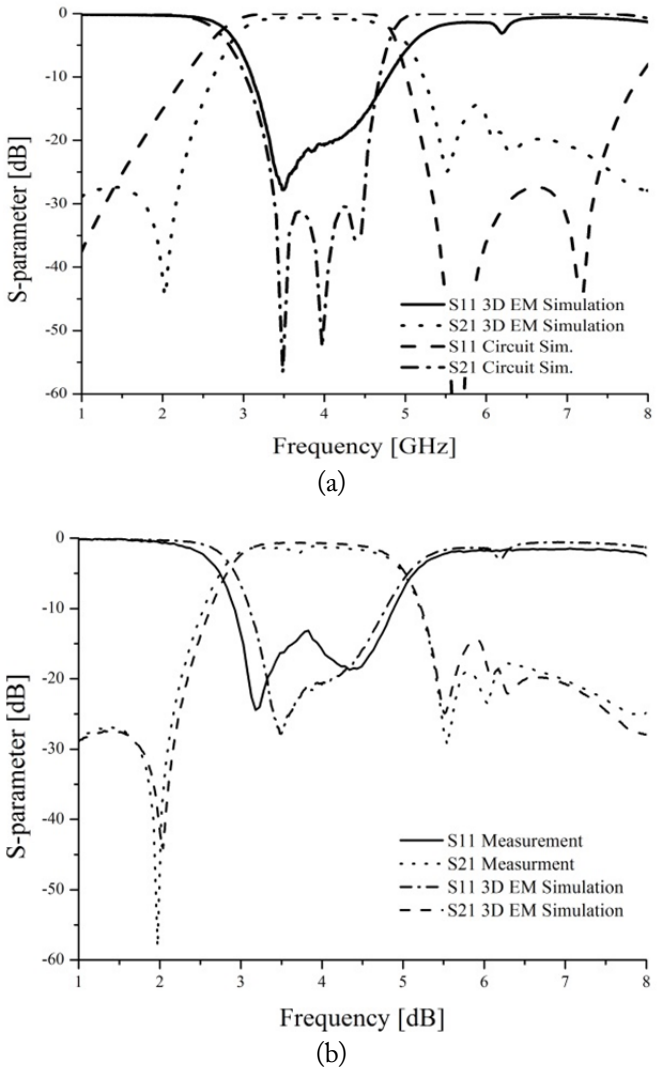

Fig. 8. S_{11} and S_{21} of the proposed band-pass filter. (a) Simulation and (b) measurement.

field and the dispersion diagram (or propagation constant vs. frequency diagram). Fig. 9(a) shows the ZOR phenomenon at f_0 (4 GHz) where the overall structure from port 1 to port 2 has almost the same electric field intensity (almost the same color means zero times the half-wavelength resonance or electric field of the same vector). Besides, seeing the dispersion curve as the relation of frequency vs. phase (= Beta × p), with respect to 4 GHz, left-handed (or minus propagation constant) and right-handed (or plus propagation constant) regions are generated below and above the ZOR point at 4 GHz. Lastly, we show the photograph of our fabricated broadband BPF to verify how the proposed design has realized miniaturization (a lot less than a quarter wavelength).

As in Figs. 7 and 10, our filter fits into the 1 × 1 cm^2 area and is less than even a quarter wavelength in area (1.83 × 1.83 cm^2), which means 54%- and greater than 70%-size reductions from the conventional quarter wavelength and half wavelength, respectively. In addition, we compared our filter with other size-

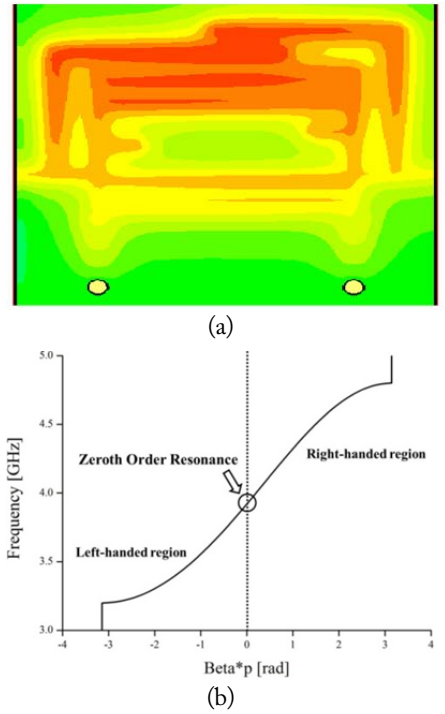

Fig. 9. Proof of the composite right- and left-handed zeroth-order resonance (CRLH ZOR) property. (a) ZOR electric field and (b) dispersion diagram.

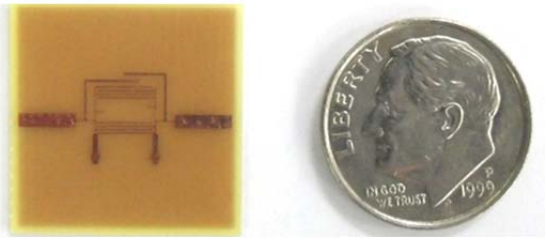

Fig. 10. Picture of the designed broadband band-pass filter.

reduced broadband structures to present the differences, features, and advantages of the proposed method.

Based on the comparison in Table 3, our structure is the shortest due to the use of the ZOR effect, which helps our design to have an insertion loss below 1 dB. In addition, it is easier to fabricate our filter compared to the defected ground in [2] and the multi-layers and metal housing in [4] now that ours is manufacturable as a printed 1-layer planar geometry.

IV. Conclusion

A new compact UWB lower-half BPF has been proposed based upon the concept of the CRLH-TL metamaterial. Only one unit of the CRLH-TL is adopted and the two pairs of inner and outer open stubs are added to form the wanted passband. After a 3D electromagnetic field simulation and fabrication, the design is validated by the measurement to show an excellent performance of the frequency response with a 3.2–4.8 GHz band, a less than 1-dB insertion loss and a less than 15-dB return loss. Lastly, the proposed design makes the overall size of the filter less than 1 × 1 cm^2 in area.

Table 3. Comparison between our and other broadband filters

	This study	Ishida and Araki [1]	Wang et al. [2]	Sun and Zhu [3]	Menzel et al. [4]
Basis of design	ZOR (CRLH)	Phase canceling (RH)	HPF + LPF (RH)	MMR (RH)	HPF + LPF (RH)
Overall size	$\ll 0.25\ \lambda_g$	$\approx \lambda_g$	$\approx \lambda_g$	$\approx 0.68\ \lambda_g$	$\approx 0.60\ \lambda_g$
Ground defect?	No	No	Yes	No	No
Shape	Split IDC blocks	Loop	0.5 λ_g TL coupled with slots	SIRs coupled with spur lines	Suspended strips
Stop-band	2 GHz	< 100 MHz	< 2 GHz	≈4 GHz	≈6 GHz
Optimized?	Yes	No	No	No	No

ZOR = zeroth-order resonance, CRLH = composite right- and left-handed, HPF = high-pass filter, LPF = low-pass filter, MMR = multi-mode resonator, IDC = interdigital coupled, SIR = stepped-impedance resonator, TL=transmitssion line.

This work was supported by the ICT R&D program of MSIP/IITP (No. 2014-044-047-001, Division of Radio Services Antenna for the Future Using a Hybrid Propagation Medium), and Mr. Kyeongnam Jang's assistance is highly appreciated.

References

[1] H. Ishida and K. Araki, "Design and analysis of UWB bandpass filter with ring filter," in *Proceedings of IEEE MTT-S International Microwave Symposium Digest*, Fort Worth, TX, 2004, pp. 1307−1310.

[2] H. Wang, L. Zhu, and W. Menzel, "Ultra-wideband band-pass filter with hybrid microstrip/CPW structure," *IEEE Microwave and Wireless Components Letters*, vol. 15, no. 12, pp. 844−846, Dec. 2005.

[3] S. Sun and L. Zhu, "Capacitive-ended interdigital coupled lines for UWB bandpass filters with improved out-of-band performances," *IEEE Microwave and Wireless Components Letters*, vol. 16, no. 8, pp. 440−442, Aug. 2006.

[4] W. Menzel, M. R. Tito, and L. Zhu, "Low-loss ultra-wideband (UWB) filters using suspended stripline," in *Proceedings of Asia-Pacific Microwave Conference*, Suzhou, China, 2005, pp. 2148−2151.

[5] C. L. Hsu, F. C. Hsu, and J. T. Kuo, "Microstrip bandpass

filters for ultra-wideband (UWB) wireless communications," in *IEEE MTT-S International Microwave Symposium Digest*, Long Beach, CA, 2005, pp. 675−678.
[6] C. Caloz and T. Itoh, *Electromagnetic Metamaterials: Transmission Line Theory and Microwave Applications.* Hoboken, NJ: John-Wiley & Sons Inc., 2006.
[7] J. Ju and S. Kahng, "A compact UWB bandpass filter using a center-tapped composite right/left-handed transmission-line zeroth-order resonator," *Microwave and Optical Technology Letters*, vol. 53, no. 9, pp. 1974−1976, Sep. 2011.
[8] S. Kahng and D. Lim, "A center-tapped CRLH ZOR UWB bandpass filter with improved stopband," *Microwave Journal*, vol. 55, no. 6, pp. 86−92, Jun. 2012.
[9] K. C. Gupta, R. Garg, I. Bahl, and P. Bhartia, *Microstrip Lines and Slotlines.* 2nd ed., Norwood, MA: Artech House Inc., 1996.

Jinsu Jeon

received his B.E. degree in August 2013, and he currently attends the graduate school program for his M.E. degree at Incheon National University in Incheon, Korea. His research fields are microwave engineering, RF components, antennas, wireless power transfer, and metamaterials. He is the recipient of the best paper at the Spring General Conference on Microwave Engineering and Antennas in May 2014 for the design of a CRLH-based, low profile 3D beam-forming antenna for V2X communication.

Sungtek Kahng

received his Ph.D. degree in electronics and communication engineering from Hanyang University, Korea in 2000, with a specialty in radio science and engineering. From 2000 to early 2004, he worked for the Electronics and Telecommunication Research Institute on numerical electromagnetic characterizations and developed RF passive components for satellites. In March 2004, he joined the Department of Information and Telecommunication Engineering at the University of Incheon, where he has continued research on analyses and advanced design methods of microwave components and antennas, including metamaterial technologies, MIMO communication, and wireless power transfer for IoE/ cyber-physical systems. In addition, he is a consultant and collaborator for Industry, the secretary of IEEE APS Korea Chapter, KIEES AP Technical Group, and the general secretary for the Korea-Japan Joint Conference on AP/EMT/EMC 2009, the Korea-Japan Microwave Workshop 2009 & 2014, GSMM 2010, APEMC 2011, ISAP 2011, and a judge for the SPC at IEEE APS 2011, 2012, and 2014. Moreover, he won the best research achievement award at the Korean Institute of Electrical Engineering in December 2014.

Hyunsoo Kim

received his B.E. degree in February 2014, and he is currently pursuing his M.E. degree at Incheon National University in Incheon, Korea. His research fields are microwave engineering, RF components, antennas, wireless power transfer, and metamaterials.